

Birhythmicity, intrinsic entrainment, and minimal chimeras in an electrochemical experiment

Juliane C. Wiehl,^{a)} Maximilian Patzauer,^{a)} and Katharina Krischer^{b)}
Nonequilibrium Chemical Physics, Department of Physics, Technical University of Munich, 85748 Garching, Germany

The coexistence of limit cycles in phase space, so called birhythmicity, is a phenomenon known to exist in many systems in various disciplines. Yet, detailed experimental investigations are rare, as are studies on the interaction between birhythmic components. In this article, we present experimental evidence for the existence of birhythmicity during the anodic electrodisso- lution of Si in a fluoride-containing electrolyte using weakly illuminated n-type Si electrodes. Moreover, we demonstrate several types of interaction between the coexisting limit cycles, in part resulting in peculiar dynamics. The two limit cycles exhibit vastly different sensitivities with respect to a small perturbation of the electrode potential, rendering the coupling essentially unidirectional. A manifestation of this is an asymmetric 1:2 intrinsic entrainment of the coexisting limit cycles on an individual uniformly oscillating electrode. In this state, the phase space structure mediates the locking of one of the oscillators to the other one across the separatrix. Furthermore, the transition scenarios from one limit cycle to the other one at the borders of the birhythmicity go along with different types of spatial symmetry breaking. Finally, the master-slave type coupling promotes two (within the experimental limits) identical electrodes initialized on the different limit cycles to adopt states of different complexity: one of the electrodes exhibits irregular, most likely chaotic, motion, while the other one exhibits period-1 oscillations. The coexistence of coherence and incoherence is the characteristic property of a chimera state, the two coupled electrodes constituting an experimental example of a smallest chimera state in a minimal network configuration.

**Bistability is both an interesting and a common phe-
nomenon in dynamical systems¹. The most common type
of bistability is the coexistence of two stable stationary
states. However, its meaning is more general and includes
the coexistence of any two attractors in phase space, such
as of a stationary state and a limit cycle, of two limit cycles,
and so on. Even bichaoticity, the coexistence of two chaotic
attractors, can occur. In this paper, we address an exper-
imental system that exhibits the coexistence of two stable
limit cycles, also referred to as birhythmicity. In a birhyth-
mic system, each of the two coexisting stable oscillatory
states can have its own frequency and amplitude, and, in
addition, might oscillate around different mean values².
While dynamic phenomena connected to the coexistence
between two stationary states, such as transitions between
them or traveling waves that might form in spatially ex-
tended systems, are well investigated³, this is not the case
for other types of bistability. Below, we demonstrate that
the two directions of the transitions between the limit cy-
cles can be of qualitatively different nature and that one
oscillation might intrinsically be influenced by the other
coexisting limit cycle, a phenomenon we refer to as intrin-
sic entrainment. Furthermore, we show that the coupling
between two birhythmic systems oscillating on different
limit cycles can be strongly asymmetric.**

I. INTRODUCTION

The discovery of birhythmicity in physical systems dates back to at least 1976, when it was reported to exist in a model of a continuous stirred tank reactor with consecutive exothermic reactions⁴. To our knowledge, the first experimental finding of birhythmicity, then called generalized multistability by the authors, was reported in 1982 in a Q -switched gas laser⁵. Later that year, Decroly and Goldbeter introduced the term birhythmicity in their theoretical study of a sequence of enzymatic reactions in a system with two positive feedback loops in series². This was one of the first attempts to characterize birhythmicity in more detail. Their approach was later used in an experimental study in which two chemical oscillators with a common intermediate were combined and the resulting system was found to exhibit birhythmicity^{6,7}. Other examples of experimental chemical systems exhibiting birhythmicity include electronic oscillators⁸, the Belousov-Zhabotinsky reaction in a stirred flow reactor⁹⁻¹¹, acetaldehyde oxidation in a continuously stirred tank reactor¹² and the gas-phase H_2+O_2 reaction in a continuously stirred tank reactor^{13,14}. Furthermore, birhythmicity proved to be important in diverse biological contexts, most notably neural activities, where examples for experimental evidences can be found e.g. in Ref. 15-17, or circadian oscillators, where an experimental demonstration is reported in Ref. 18. More recently, an experimental electrochemical example of birhythmicity has been found in the oscillatory electrodisso- lution of Cu when using a delay feedback¹⁹.

Compared to the relatively small number of experimental studies, the number of theoretical investigations on birhythmicity is much larger (see e.g. references in Ref. 1). Besides models of ordinary differential equations describing specific systems, also generic properties of spatially extended birhyth-

^{a)}These authors contributed equally to this work.

^{b)}Corresponding Author: krischer@tum.de

This is the author's peer reviewed, accepted manuscript. However, the online version of record will be different from this version once it has been copyedited and typeset.
PLEASE CITE THIS ARTICLE AS DOI: 10.1063/1.50064266

mic systems or coupled birhythmic oscillators have been studied with normal form type equations. These include wave phenomena in spatially extended reaction-diffusion models and ensembles of coupled birhythmic (phase) oscillators²⁰⁻²⁷. The latter were also found to promote the occurrence of chimera states, an interesting prediction which awaits experimental validation.

In this paper we investigate the nonlinear dynamics occurring during silicon electrodisolution in a fluoride-containing electrolyte. This system exhibits a plethora of dynamical phenomena, such as oscillations²⁸⁻³⁰, phase clusters and chemical turbulence³¹, or chimera states³². Moreover, it has been found that the system exhibits two types of limit cycles, which were coined low amplitude oscillations (LAOs) and high amplitude oscillations (HAOs), respectively³³. Although the electrochemical mechanism leading to either of these oscillations is not yet known, experiments suggested that they arise due to two different main feedback loops in the system³³. Later Tosolini et al. reported the coexistence of chaotic attractors and speculated that the bichaoticity is linked to an intrinsic birhythmicity, the interaction between the coexisting oscillators in phase space causing both of the limit cycles to become unstable and give rise to chaotic attractors³⁴. Here, we will continue on this path and show that the electrodisolution of silicon does indeed exhibit the coexistence of two stable limit cycles, yet in a drastically different parameter range than the bichaotic one.

Instead of using p-doped silicon as our working electrode as in Refs. 33 and 34, we use n-doped silicon. The electrooxidation reaction proceeds through the following net reaction:



where $1 \leq \lambda_{\text{VB}} \leq 4$ denotes the number of charge carriers that come from the valence band of the silicon. Since at least the first oxidation requires a valence band hole, the electrooxidation of n-doped Si requires the illumination of the electrode with a wavelength that is larger than the band gap. The illumination intensity is thus an additional bifurcation parameter in our study. The oxide formed in reaction (1) is chemically etched in the overall reaction³⁵



The interaction between oxidation and etching kinetics are believed to cause the oscillatory behavior³⁰, yet the corresponding feedback loops could not yet be identified.

The rest of the article is structured as follows. In section II we introduce the experimental setup. In section III we first shows the results obtained with one electrode, where birhythmicity is illustrated in phase space, physical space and in the frequency domain. Then, coupling experiments with two electrodes are presented. Implications of the experimental data concerning intrinsic and extrinsic coupling of the birhythmic system are discussed in section IV.

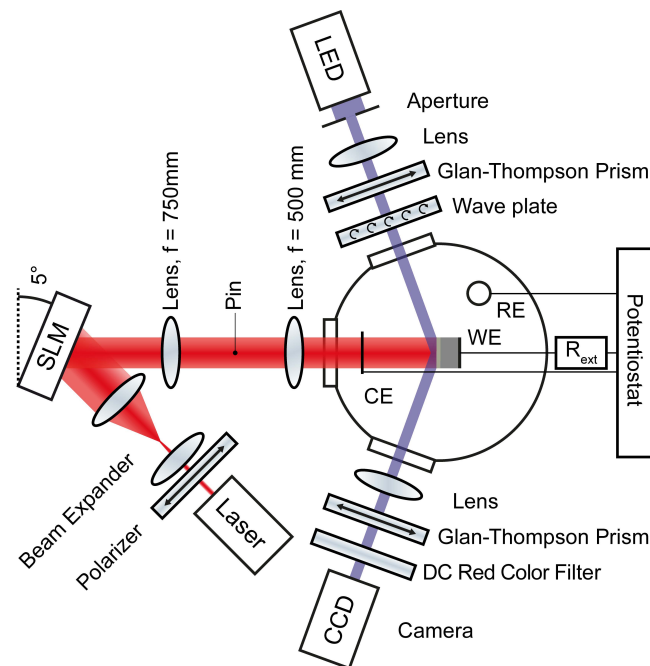


FIG. 1. Sketch of the experimental setup (not to scale) with its three parts, the laser illumination setup, with a spatial light modulator (SLM) as centerpiece, the ellipsometric imaging setup, allowing spatially resolved *in situ* monitoring of the electrode surface, and the electrochemical setup, consisting of an electrochemical cell and a potentiostat. Note that we connected a resistor R_{ext} between the working electrode (WE) and the potentiostat.

II. EXPERIMENTAL SYSTEM

The experimental setup is sketched in Fig. 1. It consisted of a three electrode cell combined with an ellipsomicroscopic imaging setup and a laser illumination setup. The working electrode (WE) was an n-doped (1-10 Ωcm) Si (111) sample. We use an external resistor with a resistance such that $R_{\text{ext}}A = 1\text{k}\Omega\text{cm}^2$, connected in series with the WE to introduce a linear global coupling to our system; this tends to synchronize the electrode surface. For the measurements with two working electrodes we placed two separate Si samples on one holder with two connecting wires which were short-circuited before the external resistor. The electrolyte (500 ml) consisted of 0.06 M NH_4F and 142 mM H_2SO_4 , was purged with argon and stirred throughout the measurements. We monitored the lateral uniformity of the electrode/electrolyte interface *in-situ* by probing the relative change in optical path length with the ellipsomicroscopic surface imaging setup^{36,37}. The resulting ellipsometric intensity signal ξ will be presented as a percentage of the saturation threshold of the recording camera. The laser illumination intensity at the electrode was controlled with a spatial light modulator (SLM) (Hamamatsu, X10468-06). The SLM ensured a uniform illumination intensity across the electrode and when two electrodes were used, it enabled us to control the illumination intensity of each electrode separately, allowing for different initialization protocols. Further experimental details can be found in the supplement.

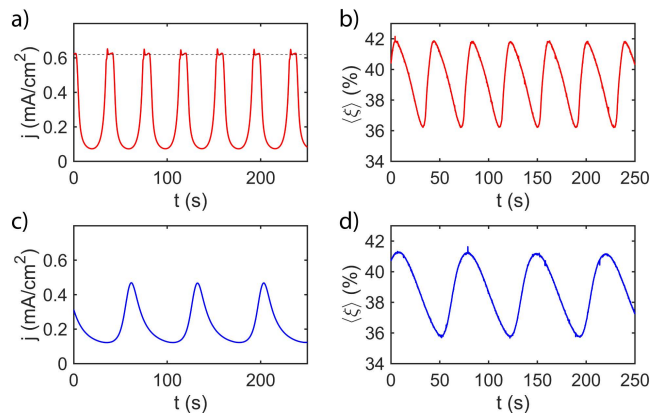


FIG. 2. Exemplary time series of an High Amplitude Oscillation (HAO), red, and of a Low Amplitude Oscillation (LAO), blue. a), c) current density j . b), d) spatially averaged ellipsometric intensity $\langle \xi \rangle$. Both oscillations were measured at $U = 6$ V vs MSE, $R_{\text{ext}}A = 1\text{ k}\Omega\text{ cm}^2$, $A = 15.72$ mm 2 , and $I_{\text{ill}} = 1.31$ mW/cm 2 .

156 tary material.

157 III. RESULTS

158 In Fig. 2 exemplary time series of the current density j and
 159 the spatially averaged ellipsometric intensity signal $\langle \xi \rangle$ of the
 160 two oscillation types found during Si electrodisolution are
 161 depicted. The oscillations shown in Fig. 2 a)-b) are HAOs
 162 and the ones in Fig. 2 c)-d) are LAOs. The most striking dif-
 163 ferences between the two oscillation types are that the HAOs
 164 have a larger amplitude of the current density and a higher
 165 frequency than the LAOs. They also differ in their shapes
 166 specifically the current of the HAOs is limited by the concen-
 167 tration of the available valence band holes during part of the
 168 oscillation. In Fig. 2 a) the current limit is indicated by a dot-
 169 ted line. We can tune this limit by changing the illumination
 170 intensity. Even though this means that the current amplitude
 171 of the HAO can be lower than the one of the LAO, we keep
 172 the naming convention introduced in the literature³³.

174 The two types of oscillations depicted in Fig. 2 were mea-
 175 sured at identical parameter values, indicating that the sys-
 176 tem is birhythmic. Thus, which oscillation type is attained
 177 depends on the initial conditions. In order to establish HAOs
 178 we performed a voltage step from the open-circuit potential
 179 to a potential in the oscillatory region (6 V vs MSE for the
 180 measurements in Fig. 2) at high illumination intensity (> 2.5
 181 mW/cm 2) and then reduced the illumination intensity to the
 182 desired intensity after the first two transient current oscilla-
 183 tions. The LAOs were initialized by performing the same po-
 184 tential jump at the same high initial illumination intensity as
 185 when initializing the HAOs. However, before lowering the il-
 186 lumination intensity to the desired value, we waited until any
 187 transients had decayed. Below we refer to these two proto-
 188 cols as the HAO- and the LAO-initialization protocols, respec-
 189 tively.

190 A. Parameter Space

191 In the following, we determine the illumination inten-
 192 sity interval in which the system exhibits birhythmicity at
 193 6 V vs MSE. Therefore, we first initialized HAOs at a low
 194 illumination intensity of 0.68 mW/cm 2 and then increased the
 195 illumination intensity stepwise. At each step we waited until
 196 any transients had died out and then recorded the oscillation.
 197 In Fig. 3 a) representative HAOs at different illumination in-
 198 tensities are shown in the $j\langle \xi \rangle$ -plane. In these phase portraits
 199 the increase in the illumination-limited current plateau with
 200 increasing illumination density becomes obvious. When we
 201 increase the illumination intensity beyond the highest illumi-
 202 nation intensity shown in Fig. 3 a) the system transitions to
 203 LAOs.

204 As we will detail below, the transition from HAOs to LAOs
 205 occurred through a nucleation and growth mechanism of the
 206 LAOs which entailed very long (≥ 2 h), spatially inhomoge-
 207 neous, transients. Therefore, we investigated the LAO branch
 208 by re-initializing LAOs according to the LAO initialization
 209 protocol. In this way, we obtained spatially uniform oscilla-
 210 tions before we lowered the illumination stepwise.

211 In Fig. 3 b) LAOs measured at the same parameters as in
 212 Fig. 3 a) are depicted. The LAOs remain spatially homoge-
 213 neous until the illumination is lowered down to 1 mW/cm 2 .
 214 For lower illumination intensities patterns emerge leading to a
 215 lower amplitude of the spatially averaged signals, as shown in
 216 Fig. 3 b). The spatial symmetry breaking at low illumination
 217 intensity confirms our previous findings^{38,39}. Comparing the
 218 location of the coexisting HAOs and LAOs in the phase-space
 219 projections in Fig. 3 a)-b), it becomes obvious that they overlap
 220 at the corresponding illumination intensity. This strongly
 221 suggests that they live in an at least three dimensional phase-
 222 space.

223 The hysteretic behavior is summarized in Fig. 3 c) where
 224 the average current densities of the oscillations are plotted
 225 versus the illumination intensity. Here, the measurement se-
 226 ries shown in red was initialized using the HAO protocol and
 227 the measurement series shown in blue was initialized using
 228 the LAO protocol, as described above. The HAO measure-
 229 ment series starts at low illumination intensities. If we follow
 230 it towards higher illumination intensities we see that the av-
 231 erage current density decreases with increasing illumination
 232 before reaching a fixed value at approx. 0.26 mA/cm 2 . The
 233 LAO measurement series starts at high illumination intensi-
 234 ties. Following it, we see that the average current density
 235 does not change with decreasing illumination intensity until
 236 the system transitions from the LAO to the HAO at an illumi-
 237 nation intensity of 0.72 mA/cm 2 .

238 Next, we will have a closer look at the transient behavior
 239 during the transition from HAOs to LAOs at high illumina-
 240 tion intensities and the transition from LAOs to HAOs at low
 241 illumination intensities.

242 A 1D cut vs. time of the evolution of ξ and three 2D snap-
 243 shots of the ellipsometric signal during the HAO \rightarrow LAO tran-
 244 sition are shown in Fig. 4 a) and b). (Multimedia view) Shortly
 245 after having increased the illumination intensity, a nucleus of
 246 the LAO appeared in the lower left part of the electrode at a

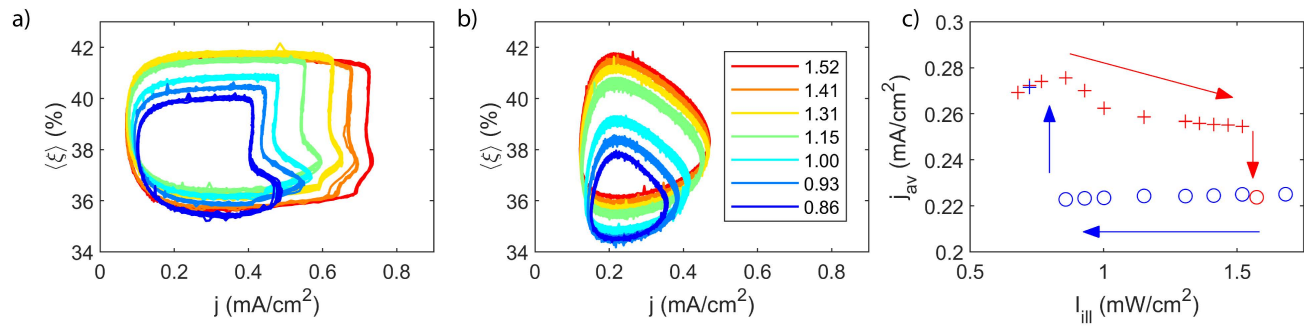


FIG. 3. Birhythmic oscillations in the $j\langle\xi\rangle$ -plane: a) HAOs and b) LAOs at different illumination intensities I_{ill} (mW/cm²) indicated by their respective color (see legend in b)). Other parameter values: 6 V vs MSE and $R_{\text{ext}}A = 1\text{k}\Omega\text{cm}^2$ with $A = 15.72\text{ mm}^2$ c) Average current density j_{av} of LAOs (o) and HAOs (+) vs illumination intensity I_{ill} for the same parameters as used in (a) and (b). The measurements of (a) and (b) are included. The arrows indicate the order of measurement. Data from two separate measurement series: Red/blue symbols indicating that the series was initialized at low/high illumination intensities and that the illumination intensity was increased/decreased stepwise (see text).

This is the author's peer reviewed, accepted manuscript. However, the online version of record will be different from this version once it has been copyedited and typeset. PLEASE CITE THIS ARTICLE AS DOI: 10.1063/5.0064266

247 point in time where the HAO current was limited, and thus
 248 very sensitive towards an increase in the hole concentration
 249 at the interface. This nucleus expands in space each time the
 250 HAO has again reached the current-limited phase. This indicates
 251 that the transition is triggered by diffusion of holes from the
 252 LAO region to the HAO region.

253 Thus, during the transition the LAO state expands in a step-
 254 like manner resulting in a striped pattern on the electrode sur-
 255 face (Fig. 4 b) (Multimedia view). The stepwise expansion
 256 can also be seen from the checkered pattern in the 1D-cut
 257 taken approximately along the direction of propagation of the
 258 LAO region. The arrangement of the squares of the checker-
 259 board pattern reflects that the ratio of the frequencies of HAOs
 260 and LAOs is approximately 2:1.

261 In contrast to this stepwise transition, the transition from
 262 a LAO to a HAO at the low illumination border is abrupt
 263 and takes place on the entire electrode at the same time. In
 264 Fig. 4 c-d) (Multimedia view) an example of such a transi-
 265 tion is shown. Once the illumination has been reduced below
 266 a critical value, the electrode attains a HAO as soon as the
 267 current reaches the new maximal current level imposed by the
 268 reduced illumination.

269 If we expand our parameter space by also changing the ap-
 270 plied voltage U , we obtain the 2D phase diagram shown in
 271 Fig. 5. Here, the HAOs are marked with crosses and the LAOs
 272 with circles. The red and blue areas indicate the regions where
 273 only HAOs respectively LAOs were found, and the striped
 274 area marks the birhythmic region. Note that we only include
 275 measurements at the edges of and not within the birhythmic
 276 region for clarity. Evidently, the birhythmic region extends
 277 over a large region in this parameter plane, demonstrating that
 278 birhythmicity is a robust feature of the system.

280 B. Frequency Domain

281 For a further characterization of the birhythmicity, it is
 282 instructive to investigate how the frequencies of HAOs and
 283 LAOs change as a function of the parameter, and in particu-
 284 lar how they behave at the transition points between the two

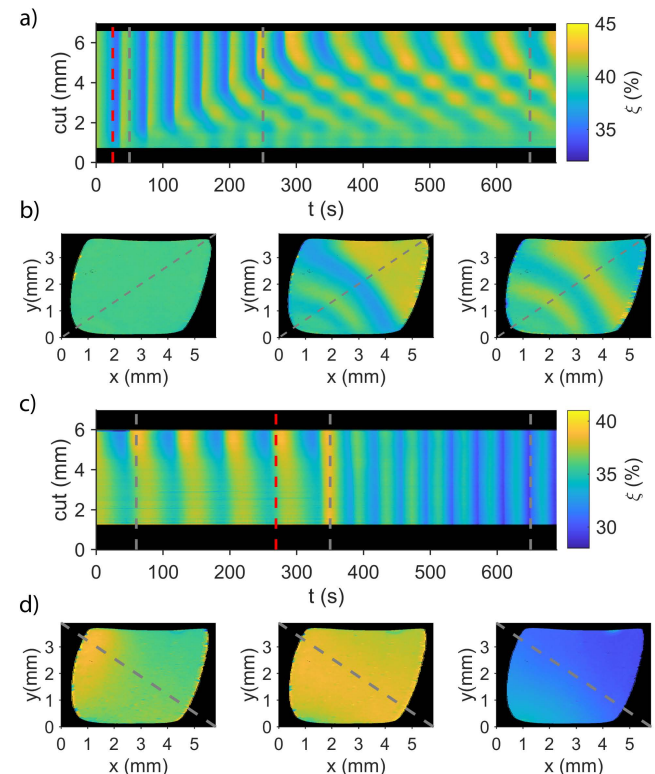


FIG. 4. Examples of the spatio-temporal dynamics at the border of the birhythmic region when the system transitions to the other oscillatory state: a)-b) high illumination (transition from HAO to LAO) and c)-d) low illumination (transition from LAO to HAO) at the same parameters as in Fig. 3 c). The dashed red lines indicate the time when the illumination intensity was changed. a) and c): Temporal evolution of the ellipsometric intensity of a 1D cut indicated by the dashed line in the leftmost snapshots in b) and d) respectively. b) and d): Snapshots of the ellipsometric intensity taken at the times indicated by the dashed gray lines in a) and c) respectively. $R_{\text{ext}}A = 1\text{ k}\Omega\text{cm}^2$ with $A = 15.72\text{ mm}^2$. (Multimedia view).

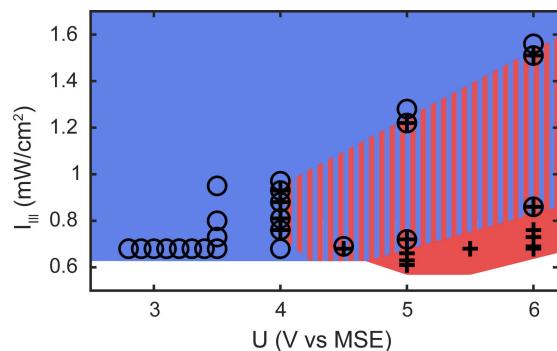


FIG. 5. Birhythmic parameter region in the U - I_{III} parameter plane: HAOs (+) and LAOs (○). Approximate existence region of HAOs (red) and LAOs (blue). The striped region indicates the birhythmic region where both oscillation types are found. For clarity only the measurements at the edges are shown in the birhythmic region. All measurements with $R_{ext}A = 1\text{k}\Omega\text{cm}^2$.

ACCEPTED MANUSCRIPT
This is the author's peer reviewed, accepted manuscript. However, the online version of record will be different from this version once it has been copyedited and typeset.
PLEASE CITE THIS ARTICLE AS DOI: 10.1063/5.0064266

oscillation forms. The easiest way to realize this is to perform a slow voltage scan while keeping the illumination intensity at a constant value. Therefore, we initialized the system at $I_{III} = 0.78\text{ mW/cm}^2$ on either side of the birhythmic region and swept the voltage slowly until a transition was observed. Then the voltage sweep was reversed and the voltage was swept back to the initial value. We used a sweep rate of $dU/dt = 0.1\text{ mV/s}$ which is slow on the time scale of the oscillations. Hence, we consider the measured quasi-stationary states to be a good representation of the true state at the respective voltages.

In Fig. 6 the resulting spectrogram of the spatially averaged ellipsometric intensity signal of two such scans are shown. Fig. 6 a) depicts an experiment that we initialized in a LAO at a low voltage, and b) one that we initialized in a HAO at high voltages. In each spectrogram the main frequency and the second frequency at each voltage are marked with a solid and a dashed line, respectively.

In the spectrogram in Fig. 6 a) we see that the main frequency of the initial LAO at 3.9 V vs MSE decreases before the system transitions to the faster oscillating HAO state at 5.8 V vs MSE. This transition from LAOs to HAOs occurs again quasi-simultaneously on the entire electrode, just as in the case when we varied the illumination, cf. Fig. 4 c)-d) (Multimedia view). As the system undergoes a transition to a HAO, the main frequency abruptly jumps from 16 mHz to 26 mHz. The frequency of the HAO first stays approximately constant and then starts to increase at about 5 V vs MSE. The increase in frequency is accompanied by the emergence of subharmonic mode.

We observe a similar behavior when the system is initialized in a HAO state and the voltage is swept towards lower values (Fig. 6 b)). First, the frequency hardly changes with decreasing voltage until at about 5 V vs MSE where it starts to increase and a first subharmonic peak emerges. In a small voltage interval around 4 V vs MSE this first subharmonic peak is accompanied by a sub-subharmonic frequency. The emergence of the subharmonic frequencies is accompanied by

a spatial symmetry breaking and the electrode tends to exhibit antiphase behavior. These phase-cluster-type patterns disappear again at lower potentials, before the system transitions into the LAO state at 4 V vs MSE. Interestingly, at this transition the subharmonic frequency of the HAO matches the main frequency of the LAO and, accordingly, the main frequency of the HAO matches the first superharmonic frequency of the LAO. The appearance of the subharmonic frequency during the HAOs and the 1:2 frequency ratio of LAOs and HAOs at the HAO→LAO transition could be linked to a mutual influence of the two oscillations in phase space. We will come back to this point below.

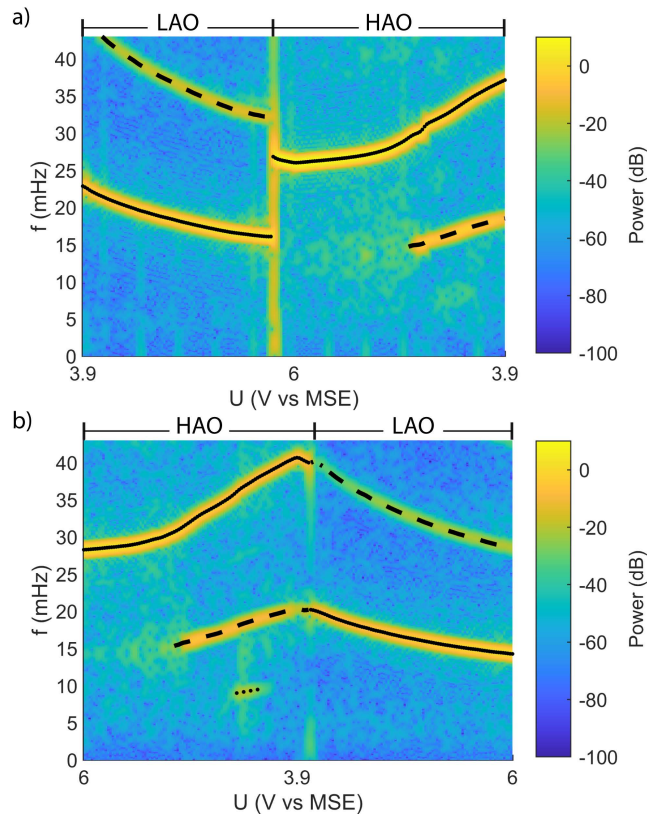


FIG. 6. Spectrogram of the spatially averaged ellipsometric intensity signal (ξ) from quasi-stationary cyclic voltammogram ($dU/dt = 0.1\text{ mV/s}$) at illumination intensity $I_{III} = 0.78\text{ mW/cm}^2$. The solid line indicates the main frequency, the dashed line indicates the second frequency, and the dotted line indicates the third frequency. a) System initialized in a LAO state at 3.9 V vs MSE. b) System initialized in a HAO state at 6 V vs MSE. Both measurements with $R_{ext}A = 1\text{k}\Omega\text{cm}^2$ and with $A = 17.51\text{ mm}^2$ in a) and $A = 16.69\text{ mm}^2$ in b).

C. Two Electrodes

To better understand how HAOs and LAOs influence each other, we will now look at what happens when we split the working electrode into two smaller electrodes and couple them through a common external resistor. Due to this cou-

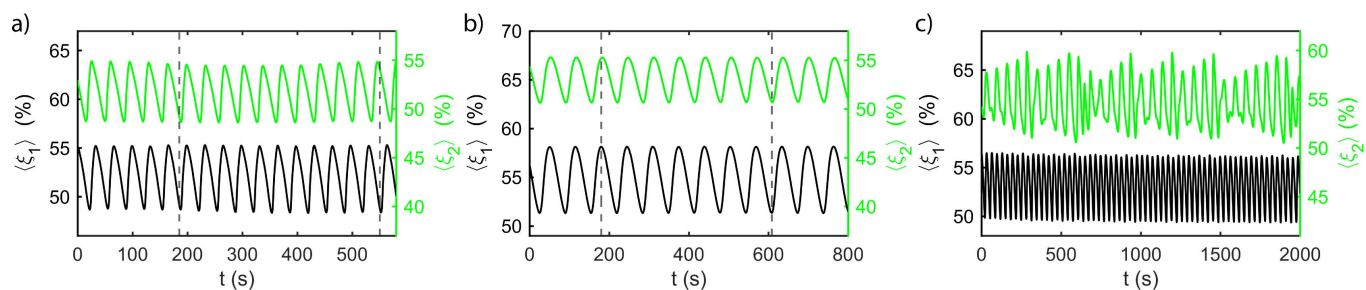


FIG. 7. Exemplary time series of the spatially averaged ellipsometric intensity of two electrodes coupled electrically through an external resistor. a) Both electrode 1 $\langle \xi_1 \rangle$ and electrode 2 $\langle \xi_2 \rangle$ in a HAO state. b) Both electrodes in an LAO state. c) Electrode 1 in a HAO state and electrode 2 in a chaotic state. Here, electrode 2 was initialized using the LAO-initialization protocol. $A_1 = 11.43 \text{ mm}^2$, $A_2 = 10.55 \text{ mm}^2$. $R_{\text{ext}}(A_1 + A_2) = 1 \text{ k}\Omega\text{cm}^2$, $I_{\text{III}} = 1.0 \text{ mW/cm}^2$, $U = 5.75 \text{ V vs MSE}$. (Multimedia view).

342 pling, any change in current at one electrode causes the poten-383
343 tial drops across both electrode/electrolyte interfaces $U_{\text{el},1/2}$ 384
344 to change according to: 385

$$345 \quad U_{\text{el},1} = U_{\text{el},2} = U - R_{\text{ext}}(j_1 A_1 + j_2 A_2), \quad (3)_{386}$$

346 where U is the externally applied voltage, and $j_{1/2}$ and $A_{1/2}$
347 are the current densities and areas of the respective electrodes.
348 The use of the SLM allows us to employ different initializa-
349 tion protocols to the two electrodes so that we can initial-388
350 ize each electrode in either a HAO or a LAO state indepen-389
351 dently. In Fig. 7 (Multimedia view) the resulting time series-390
352 of the spatially averaged ellipsometric intensity of the respec-391
353 tive electrodes are shown for three different cases. All three-392
354 cases were measured at the same parameters, they only dif-393
355 fer in the initialization protocol. Note that both electrodes re-394
356 main essentially spatially homogeneous, except of the LAO-395
357 initialized electrode of case c) where minor spatial wave-like-396
358 patterns emerged. 397

359 Fig. 7 a) (Multimedia view) depicts time series of the two-398
360 electrodes when they are both initialized with the HAO proto-399
361 col. It can be seen that the oscillations on the two electrodes-400
362 are slightly out of phase at $t = 0 \text{ s}$, are in phase at $t = 185 \text{ s}$,
363 and have drifted to an antiphase configuration at $t = 550 \text{ s}$.
364 Clearly, the slightly different parameters of the two electrodes-403
365 (such as a minor difference in their electrode areas) lead to
366 small difference of their natural frequencies, and the coupling-405
367 via the external resistor does not suffice to synchronize them.
368

369 The picture is different in the case of the LAOs. When we-407
370 initialize both electrodes using the LAO protocol, they typi-408
371 cally exhibit phase synchronization, as can be seen in Fig. 7 b)-409
372 (Multimedia view). 410

373 Fig. 7 c) (Multimedia view) depicts an example where elec-411
374 trode 1 was initialized with the HAO protocol and electrode 2-412
375 with the LAO protocol. In this case, electrode 1 assumes
376 periodic HAO which is very close to the one of case a). In-414
377 contrast, electrode 2 does not oscillate in a simple periodic-415
378 LAO state. Instead it exhibits a more complex temporal be-416
379 havior. The frequency spectrum of the time series (not shown)-417
380 exhibits a strongly enhanced background distribution around-418
381 the main oscillation frequency, suggesting that the dynamics-419
382 is chaotic. 420

382 This counterintuitive coexistence of chaos and order is no-422

only stable under these exact conditions but it persists for a
wide range of potentials. When initializing the two electrodes
in the same way as in Fig. 7 c) (Multimedia view) and then
performing a quasi-static cyclic sweep of the applied potential
we obtain the two spectrograms shown in Fig. 8.

Again, the sweep rate was slow ($dU/dt = 0.1 \text{ mV/s}$) on the
time scale of the oscillations and we assume that the measured
states are in good agreement with the true state at the respec-
tive parameters. Fig. 8 a) shows the corresponding spectrogram
of the electrode that was initialized with the HAO proto-
col. The electrode oscillates in a HAO state and behaves
similarly to a single electrode under the same conditions, cf.
Fig. 6 a). The only difference is that the subharmonic fre-
quency is active in the entire existence region of the HAOs,
not just from approximately 5 V vs MSE downwards. Fig. 8 b)
shows the spectrogram of the electrode that was initialized
according to the LAO protocol. This spectrogram differs sig-
nificantly from the case with only one electrode, cf. Fig. 6 b).
Here, we can see a broad potential region between 6 V vs MSE
and approximately 4.9 V vs MSE, indicated by the dashed red
line, where the power spectrum exhibits a strongly enhanced
background and is smeared out around the main frequency
and the first superharmonic frequency. This is a manifesta-
tion of the temporally complex behavior. Hence, we have
a large region in parameter space in which we find the co-
existence of a periodic HAO on one electrode and complex,
most likely chaotic oscillations on the other one. For poten-
tials beyond the dashed red line the spectrogram of electrode 2
becomes narrower again before the superharmonic frequency
disappears at the same voltage at which electrode 1 transi-
tions from the HAO to the LAO. In this intermediate region
the HAOs and LAOs on the two electrodes exhibit a 2:1 lock-
ing. After the transition of electrode 1 to the LAO state both
electrodes exhibit phase-synchronized LAOs. The reason for
the slightly lower power after the transition is that patterns
form on both electrodes, suppressing the amplitude of the spa-
tially averaged signal. Once the electrodes become spatially
more uniform again, the superharmonic peak in the spectrum
becomes visible again, too.

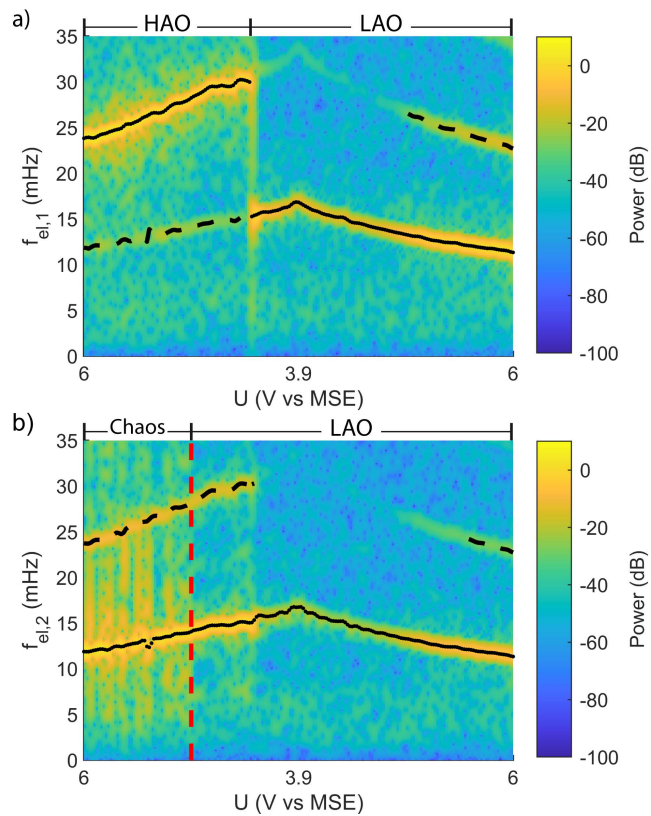


FIG. 8. Spectrograms of two coupled electrodes, obtained from the spatially averaged ellipsometric intensity signal and a quasi-stationary cyclic voltage scan ($dU/dt = 0.1$ mV/s) at illumination intensity $I_{\text{ill}} = 0.94$ mW/cm² and $R_{\text{ext}}(A_1 + A_2) = 1$ k Ω cm². The solid line indicates the main frequency and the dashed line indicates the second frequency. a) Electrode 1, initialized with the HAO protocol, $A_1 = 5.53$ mm². b) Electrode 2, initialized with the LAO protocol, $A_2 = 6.17$ mm².

IV. DISCUSSION

We presented clear-cut experimental evidence that the electrode dissolution of silicon in fluoride containing electrolyte exhibits birhythmicity. Besides this observation, our experiments elucidated unusual, though general ways, in which existing limit cycles can interact with each other. In the following we take a closer look at these interactions. We discriminate here between an *extrinsic* interaction of (nearly) identical birhythmic systems, and an *intrinsic* interaction of the two limit cycles in phase space.

The extrinsic coupling mechanism is the one easier to rationalize. We will therefore discuss it first. Consider again the results depicted in Fig. 7 (Multimedia view). Here, we coupled two nearly identical Si electrodes through an external resistor. Hence, the coupling acts, as obvious from Eq. (3), on the potential drops across the interface of the electrodes. The fact that the oscillations of the two electrodes phase-synchronize when they are both initialized with the LAO protocol but that the phases of the oscillations remain drifting when the electrodes are initialized with the HAO protocol reveal that the

sensitivity of HAOs and LAOs towards perturbations in the potential is vastly different. The experiment, where the two electrodes were initialized in different states, shows that the impact of the electrode initialized in an LAO on the one initialized in an HAO is negligible, while the other way round the dynamics of the LAO initialized electrode is strongly forced by the electrode in the HAO state. Thus, the mutual interactions of the two types of oscillations is unidirectional, i.e., of the master-slave type.

The phase-space portraits depicted in Fig. 3 shed light on this unidirectional coupling. The phase portraits of the two limit cycles intersect in the $j\langle\xi\rangle$ -phase-space plane suggesting that the oscillations live in a phase space spanned by at least three essential variables. The sensitivity of the LAO with respect to changes in the electrode potential indicates that the electrode potential is an essential variable for the LAOs. Contrary, from the insensitivity of the HAOs upon variations of the electrode potential we can conjecture that the HAO limit cycle occupies a subspace of phase space that is orthogonal to the electrode potential axis. Yet, since during HAOs the current oscillates, the coupling through the resistor changes the electrode potential of both electrodes. The oscillating electrode potential acts like a periodic forcing on the LAO, while it is like an 'invariant' parameter for the HAO.

The coupling experiments presented in Fig. 3 c) were carried out at 5.75 V vs MSE. The spectrograms in Fig. 6 confirm, that approx. between 6 and 5 V vs MSE the HAO frequency is essentially independent of the applied voltage.

This changes at lower voltages, where we will argue that an intrinsic coupling comes into play. Here, the HAO frequency increases considerably, and, more strikingly, a subharmonic frequency emerges. The corresponding time series of the current and the average ellipsometric signal exhibit the typical signature of a period doubling bifurcation, i.e. increasing differences in the maxima and minima of successive oscillations with decreasing voltage. This corroborates that the system lives in at least a 3-dimensional phase space. More importantly, the subharmonic frequency coincides almost perfectly with the frequency of the LAO, at least at the HAO→LAO transition (see Fig. 6 b)). It appears likely that this is not a coincidence but rather that the existence of the LAO in phase space triggers the period doubling bifurcation. In other words, the HAO is intrinsically entrained to the LAOs in a 2:1 resonance.

A possible scenario would be as follows: Recall that also here the working electrode is connected to the potentiostat via an external resistor. Thus, the oscillating current during HAOs causes an oscillating electrode potential. Above we have discussed that these changes in the electrode potential affect the LAOs in a second electrode. For an individual electrode, the LAO exist somewhere else in phase space. Yet, the phase space structure can be such that the oscillatory motion of the LAO is felt also on the other side of the separatrix where initial conditions relax to the HAO. Hence, the oscillatory potential will induce an oscillatory motion in the plane spanned by the essential variables of the LAOs. We have argued above that one of these variables is the electrode potential upon which the HAOs are insensitive. HAOs could, how-

This is the author's peer reviewed, accepted manuscript. However, the online version of record will be different from this version once it has been copyedited and typeset.
PLEASE CITE THIS ARTICLE AS DOI: 10.1063/1.50064266

501 ever, be sensitive, on changes in the second essential LAO⁵⁵⁹
502 variable. Then, we can interpret the period doubling of the⁵⁶⁰
503 HAO as being caused by an intrinsic entrainment originating⁵⁶¹
504 from the coexisting LAOs.⁵⁶²

505 Note that in addition, at potentials lower than approx⁵⁶³
506 4 V vs MSE the HAOs might become more sensitive agains⁵⁶⁴
507 perturbations in the electrode potential than they are at high⁵⁶⁵
508 potentials. We have seen that the LAOs are sensitive toward⁵⁶⁶
509 the concentration of holes at the Si/SiO₂ interface. At high⁵⁶⁷
510 potentials, the potential drop across the space charge layer is⁵⁶⁸
511 large and the space charge layer very compact such that nearly⁵⁶⁹
512 all holes that are generated by the illumination in the bulk of⁵⁷⁰
513 the Si are quickly drawn to the Si/SiO₂ interface. Their con-⁵⁷¹
514 centration thus remains unaffected by the externally applied⁵⁷²
515 voltage. At lower voltages, however, some of the holes will⁵⁷³
516 recombine with electrons before reaching the surface. The⁵⁷⁴
517 fraction of holes which is lost due to recombination is large⁵⁷⁵
518 the lower the voltage is. At present, we do not know whethe⁵⁷⁶
519 the mechanism leads to an appreciable change in hole concen-⁵⁷⁷
520 tration at the interface. If it does, it would lead to a sensitivity⁵⁷⁸
521 change of the HAOs towards changes in the potential. How⁵⁷⁹
522 ever, independently of the sensitivity of the HAOs toward⁵⁸⁰
523 perturbations in the electrode potential, the occurrence of ⁵⁸¹
524 2:1 resonance still seems to require that the HAOs couple to⁵⁸²
525 the motion of the LAOs - most likely involving a second vari-⁵⁸³
526 able.⁵⁸⁴

527 The different sensitivity of HAOs and LAOs on perturba-⁵⁸⁵
528 tions in different variables also explains the different nature⁵⁸⁶
529 of the transitions HAO→LAO and LAO→HAO (cf. Fig. 4)⁵⁸⁷
530 (Multimedia view):⁵⁸⁸

531 Let us first look at the HAO→LAO transition, which occurs⁵⁸⁹
532 through a nucleation and growth mechanism. We can assume⁵⁹⁰
533 that the growth of the LAO domain is mediated via diffusion⁵⁹¹
534 of valence band holes. Every time the HAO is on the curren⁵⁹²
535 limited plateau, diffusion of holes from the LAO covered re-⁵⁹³
536 gion to the HAO region triggers a transition from the HAO to⁵⁹⁴
537 the LAO close to the boundary between the two oscillations.⁵⁹⁵
538 Thus, the propagation velocity of the LAO region is deter-⁵⁹⁶
539 mined by a combination of the limited (nonlocal, see Refs. 38⁵⁹⁷
540 and 39) diffusion length of the holes and the oscillation fre-⁵⁹⁸
541 quency of the HAOs.⁵⁹⁹

542 In contrast, the LAO→HAO transition takes place on the
543 entire electrode at almost exactly the same time. This fast
544 transition indicates that the coupling has a nearly global range.⁶⁰⁰
545 Considering that the external resistor introduces a global cou-
546 pling on the potential and the fact that the LAOs are very sen-⁶⁰¹
547 sitive to changes in the potential, it is most likely that this spa-⁶⁰²
548 tially uniform transition is triggered through a perturbation in⁶⁰³
549 the potential that lifts the LAO on the entire electrode across⁶⁰⁴
550 the separatrix.⁶⁰⁵

551 Finally, let us turn again to the two coupled electrodes,⁶⁰⁶
552 where one electrode was initiated in the HAO state and the⁶⁰⁷
553 other in the LAO state (Fig. 7 c) (Multimedia view). These dy-⁶⁰⁸
554 namics are very similar to the smallest chimera state as found⁶⁰⁹
555 as solutions in a chemical model of two coupled identical uni-⁶¹⁰
556 modal oscillators^{40,41}. Similar to our results, the simulation⁶¹¹
557 shows one oscillator exhibiting regular oscillations while the⁶¹²
558 other one exhibited chaotic oscillations. To the best of our⁶¹³

knowledge, we present here the first experimental realization
of a smallest chimera state consisting of only two coupled os-
cillators. Furthermore, the authors of Refs. 40 and 41 at-
tributed this particular type of chimera state to a master-slave-
type coupling. The authors argue that in their case this cou-
pling was generated by a canard explosion. We present evi-
dence that in our case the effective unidirectional coupling
comes about by the widely different sensitivities of the two
birhythmic limit cycles with respect to the coupling variables.

Yet, we note that at this stage it is unclear whether the
chaotic behavior of the LAO initialized electrode can be fully
explained by the unidirectional coupling. The dynamics is
further complicated by the fact that the forcing of the LAO by
the HAO increases the maximal current density of the LAO
such that it reaches the illumination-limited current level.
It has been shown that when an LAO comes close to the
illumination-limited current level, the electrode tends to form
spatial structures^{38,39}. Here, too, the electrode does not re-
main completely uniform but tends to form fast spreading
waves. We also note that the chaotic behavior exists only in
the voltage interval between 6 and 5 V vs MSE, as indicated
by the red-dashed line in Fig. 8 b). For lower voltages the os-
cillations initialized with the LAO protocol exhibit a 1:2 lock-
ing to the HAO, until the HAOs transition to LAOs at about
4.3 V vs MSE.

A connection between birhythmic systems and chimera
states has also been discussed in the context of ensembles of
coupled oscillators^{26,27}. Ref. 27 considered a model of non-
locally coupled birhythmic oscillators and found that the os-
cillators could organize themselves in synchronized domains
separated by asynchronous domains. Also in ensembles of
birhythmic Stuart-Landau-type as well as phase oscillators
chimera state were reported to exist²⁶.

With the present system, it might be possible to experimen-
tally validate some of these theoretical studies. Furthermore,
when changing the perspective and viewing the system of two
coupled electrodes not as a system consisting of two individ-
ual units but instead regarding each subsystem as an oscilla-
tory medium with many coupled degrees of freedom, then a
large variety of possibilities opens up to investigate pattern
formation in coupled networks experimentally.

V. CONCLUSION

In this study, we confirmed that there are two different types
of current oscillations during silicon electrodisolution. We
explicitly showed that, for a broad range of parameters, these
oscillation types are bistable, i.e. the system exhibits birhyth-
micity. Furthermore, we were able to identify three dynamical
properties that are closely related to the birhythmic nature
of the system: (1) An *intrinsic* entrainment of the motion of
one oscillator to the motion of the other one, mediated by the
vector field in phase space. (2) A unidirectional or master-
slave type coupling of two identical oscillatory systems. This
behavior is linked to the possibility that the two limit cycles
exhibit pronouncedly different sensitivities towards the per-
turbation in a variable. (3) The existence of a stable state of

614 two coupled, identical electrodes where one electrode oscillates chaotically and the other one periodically, illustrating a route to a two oscillator minimal chimera state.

617 Currently, we are only in the beginning of understanding coupled birhythmic systems. The present system promises to become a prototypical experimental model system for studies of birhythmic dynamics. The very property that distinguishes the present system from other ones is that the initial conditions can be easily controlled both in time and space, allowing to select each location - or coupled electrode - in the chosen oscillation type.

625 DATA AVAILABILITY STATEMENT

626 The data that support the findings of this study are available from the corresponding author upon reasonable request.

628 SUPPLEMENTARY MATERIAL

629 See supplemental material for a detailed explanation of the experimental setup and for complementary videos showing the dynamics presented in Fig. 4 and Fig. 7.

632 ACKNOWLEDGMENTS

633 The authors thank Sindre W. Haugland and Munir M. Salman for fruitful discussions and are grateful to Richard Hueck for his preliminary experimental work and to Anton Tosolini for his help with the installation of the spatial light modulator. The project was funded by the Deutsche Forschungsgemeinschaft (DFG, German Research Foundation) project KR1189/18 "Chimera States and Beyond".

640 REFERENCES

- 641 ¹A. N. Pisarchik and U. Feudel, "Control of multistability," *Phys. Rep.* **540**, 167–218 (2014).
 642
 643 ²O. Decroly and A. Goldbeter, "Birhythmicity, chaos, and other patterns of temporal self-organization in a multiply regulated biochemical system," *Proc. Natl. Acad. Sci.* **79**, 6917–6921 (1982).
 644
 645 ³A. S. Mikhailov, *Foundations of Synergetics I Distributed Active Systems*, Springer Series in Synergetics, Vol. 51 (Springer Berlin Heidelberg, Berlin Heidelberg, 1994).
 646
 647 ⁴D. S. Cohen and J. P. Keener, "Multiplicity and stability of oscillatory states in a continuous stirred tank reactor with exothermic consecutive reactions A B C," *Chem. Eng. Sci.* **31**, 115–122 (1976).
 648
 649 ⁵F. T. Arecchi, R. Meucci, G. Puccioni, and J. Tredicce, "Experimental evidence of subharmonic bifurcations, multistability, and turbulence in a Q-switched gas laser," *Phys. Rev. Lett.* **49**, 1217–1220 (1982).
 650
 651 ⁶M. Alamgir and I. R. Epstein, "Birhythmicity and compound oscillations in coupled chemical oscillators: Chlorite-bromate-iodide system," *J. Am. Chem. Soc.* **105**, 2500–2502 (1983).
 652
 653 ⁷M. Alamgir and I. R. Epstein, "Systematic design of chemical oscillators, Part 19. Experimental study of complex dynamical behavior in coupled chemical oscillators," *J. Phys. Chem.* **88**, 2848–2851 (1984).

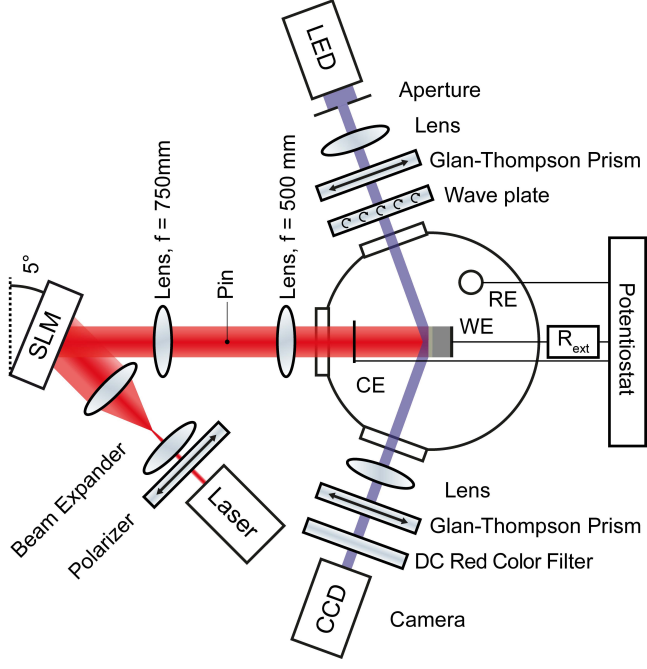
- ⁸D. Biswas, T. Banerjee, and J. Kurths, "Control of birhythmicity through conjugate self-feedback: Theory and experiment," *Phys. Rev. E* **94**, 1–7 (2016).
⁹J.-C. Roux, "Experimental studies of bifurcations leading to chaos in the Belousov-Zhabotinsky reaction," *Phys. D Nonlinear Phenom.* **7**, 57–68 (1983).
¹⁰P. Lamba and J. L. Hudson, "Experimental evidence of multiple oscillatory states in a continuous reactor," *Chem. Eng. Commun.* **32**, 369–375 (1985).
¹¹J. Maselko and H. L. Swinney, "Complex periodic oscillations and Farey arithmetic in the Belousov-Zhabotinskii reaction," *J. Chem. Phys.* **85**, 6430–6441 (1986).
¹²B. Gray and J. Jones, "The heat release rates and cool flames of acetaldehyde oxidation in a continuously stirred tank reactor," *Combust. Flame* **57**, 3–14 (1984).
¹³D. Baulch, J. F. Griffiths, A. J. Pappin, and A. F. Sykes, "Stationary-state and oscillatory combustion of hydrogen in a well-stirred flow reactor," *Combust. Flame* **73**, 163–185 (1988).
¹⁴B. R. Johnson, J. F. Griffiths, and S. K. Scott, "Characterisation of oscillations in the H₂ + O₂ reaction in a continuous-flow reactor," *J. Chem. Soc. Faraday Trans.* **87**, 523–533 (1991).
¹⁵H. A. Lechner, D. A. Baxter, J. W. Clark, and J. H. Byrne, "Bistability and its regulation by serotonin in the endogenously bursting neuron R15 in Aplysia," *J. Neurophysiol.* **75**, 957–962 (1996).
¹⁶H. Jahnsen and R. Llinás, "Ionic basis for the electro-responsiveness and oscillatory properties of guinea-pig thalamic neurones in vitro," *J. Physiol.* **349**, 227–247 (1984).
¹⁷J. Hounsgaard, H. Hultborn, B. Jespersen, and O. Kiehn, "Bistability of alpha-motoneurons in the decerebrate cat and in the acute spinal cat after intravenous 5-hydroxytryptophan," *J. Physiol.* **405**, 345–367 (1988).
¹⁸J. S. Pendergast, K. D. Niswender, and S. Yamazaki, "The complex relationship between the light-entrainable and methamphetamine-sensitive circadian oscillators: Evidence from behavioral studies of Period-mutant mice," *Eur. J. Neurosci.* **38**, 3044–3053 (2013).
¹⁹T. Nagy, E. Verner, V. Gáspár, H. Kori, and I. Z. Kiss, "Delayed feedback induced multirhythmicity in the oscillatory electrodisolution of copper," *Chaos* **25**, 064608 (2015).
²⁰D. Battogtokh and J. J. Tyson, "Turbulence near cyclic fold bifurcations in birhythmic media," *Phys. Rev. E - Stat. Physics, Plasmas, Fluids, Relat. Interdiscip. Top.* **70**, 7 (2004).
²¹M. Stich, M. Ipsen, and A. S. Mikhailov, "Self-organized stable pacemakers near the onset of birhythmicity," *Phys. Rev. Lett.* **86**, 4406–4409 (2001).
²²M. Stich, M. Ipsen, and A. S. Mikhailov, "Self-organized pacemakers in birhythmic media," *Phys. D Nonlinear Phenom.* **171**, 19–40 (2002).
²³R. Yamapi, G. Filatella, and M. A. Aziz-Alaoui, "Global stability analysis of birhythmicity in a self-sustained oscillator," *Chaos* **20**, 013114 (2010).
²⁴D. Biswas, T. Banerjee, and J. Kurths, "Control of birhythmicity: A self-feedback approach," *Chaos* **27**, 063110 (2017).
²⁵O. V. Astakhov, S. V. Astakhov, N. S. Krakhovskaya, V. V. Astakhov, and J. Kurths, "The emergence of multistability and chaos in a two-mode van der Pol generator versus different connection types of linear oscillators," *Chaos* **063118**, 063118 (2018).
²⁶A. Yeldesbay, A. Pikovsky, and M. Rosenblum, "Chimeralike states in an ensemble of globally coupled oscillators," *Phys. Rev. Lett.* **112**, 144103 (2014).
²⁷A. Provata, "Chimera states formed via a two-level synchronization mechanism," *J. Phys. Complex.* **1**, 025006 (2020).
²⁸D. R. Turner, "Electropolishing silicon in hydrofluoric acid solutions," *J. Electrochem. Soc.* **105**, 402 (1958).
²⁹V. Lehmann, "The physics of macropore formation in low doped n-type silicon," *J. Electrochem. Soc.* **140**, 2836 (1993).
³⁰X. G. Zhang, *Electrochemistry of Silicon and Its Oxide* (Kluwer Academic Publishers, Boston, 2004) p. 510.
³¹K. Schönleber, C. Zensen, A. Heinrich, and K. Krischer, "Pattern formation during the oscillatory photoelectrodisolution of n-type silicon: Turbulence, clusters and chimeras," *New Journal of Physics* **16**, 63024 (2014).
³²L. Schmidt, K. Schönleber, K. Krischer, and V. García-Morales, "Coexistence of synchrony and incoherence in oscillatory media under nonlinear global coupling," *Chaos* **24**, 013102 (2014).
³³K. Schönleber and K. Krischer, "High-amplitude versus low-amplitude current oscillations during the anodic oxidation of p-type silicon in fluoride

This is the author's peer reviewed, accepted manuscript. However, the online version of record will be different from this version once it has been copyedited and typeset.

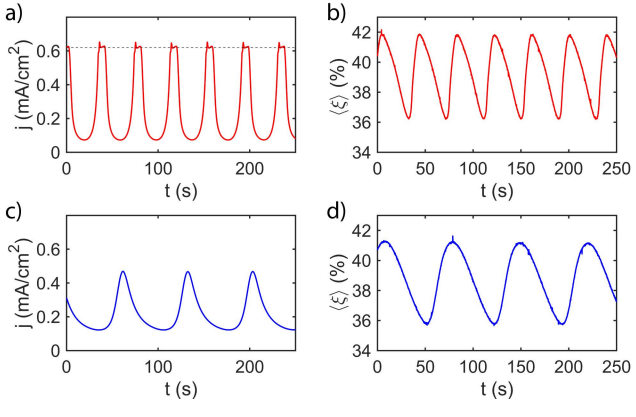
PLEASE CITE THIS ARTICLE AS DOI: 10.1063/5.0064266

- 731 containing electrolytes," *ChemPhysChem* **13**, 2989–2996 (2012). 744
- 732 ³⁴A. Tosolini, M. Patzauer, and K. Krischer, "Bichaoticity induced by in-745
733 herent birhythmicity during the oscillatory electrodisso-746
734 *Chaos* **29**, 043127 (2019). 747
- 735 ³⁵S. Cattarin, I. Frateur, M. Musiani, and B. Tribollet, "Electrodissolution of 748
736 p-Si in acidic fluoride media modeling of the steady state," *J. Electrochem* 749
737 *Soc.* **147**, 3277 (2000). 750
- 738 ³⁶H. H. Rotermund, G. Haas, R. U. Franz, R. M. Tromp, and G. Ertl, "Imag-751
739 ing pattern formation in surface reactions from ultrahigh vacuum up to at-752
740 mospheric pressures," *Science* **270**, 608–610 (1995). 753
- 741 ³⁷I. Miethe, V. García-Morales, and K. Krischer, "Irregular subharmonic clus-754
742 ter patterns in an autonomous photoelectrochemical oscillator," *Phys. Rev* 755
743 *Lett.* **102**, 194101 (2009).
- ³⁸M. Patzauer, R. Hueck, A. Tosolini, K. Schönleber, and K. Krischer, "Au-
tonomous oscillations and pattern formation with zero external resistance
during silicon electrodisso-
lution," *Electrochim. Acta* **246**, 315–321 (2017).
- ³⁹M. Patzauer and K. Krischer, "Self-organized multifrequency clusters in an
oscillating electrochemical system with strong nonlinear coupling," *Phys.*
Rev. Lett. **126**, 194101 (2021).
- ⁴⁰N. M. Awal, D. Bullara, and I. R. Epstein, "The smallest chimera: Periodic-
ity and chaos in a pair of coupled chemical oscillators," *Chaos* **29**, 013131
(2019).
- ⁴¹N. M. Awal and I. R. Epstein, "Post-canard symmetry breaking and other
exotic dynamic behaviors in identical coupled chemical oscillators," *Phys.*
Rev. E **101**, 042222 (2020).

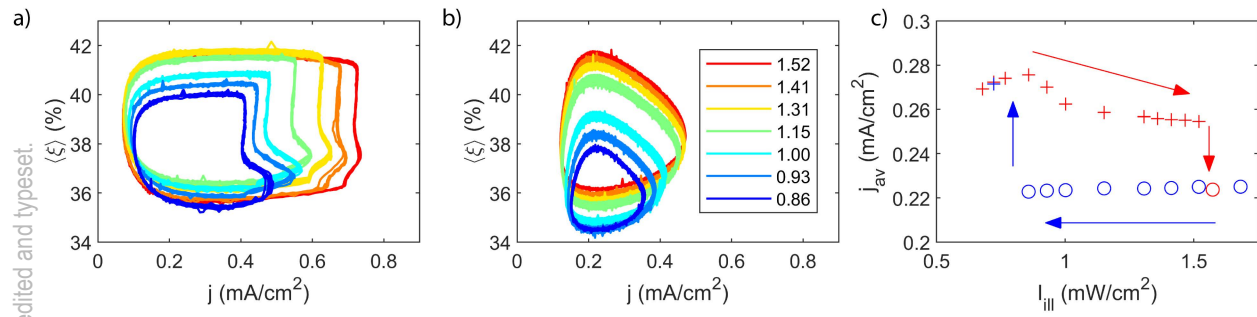
This is the author's peer reviewed, accepted manuscript. However, the online version of record will be different from this version once it has been copyedited and typeset.
 PLEASE CITE THIS ARTICLE AS DOI: 10.1063/5.0064266



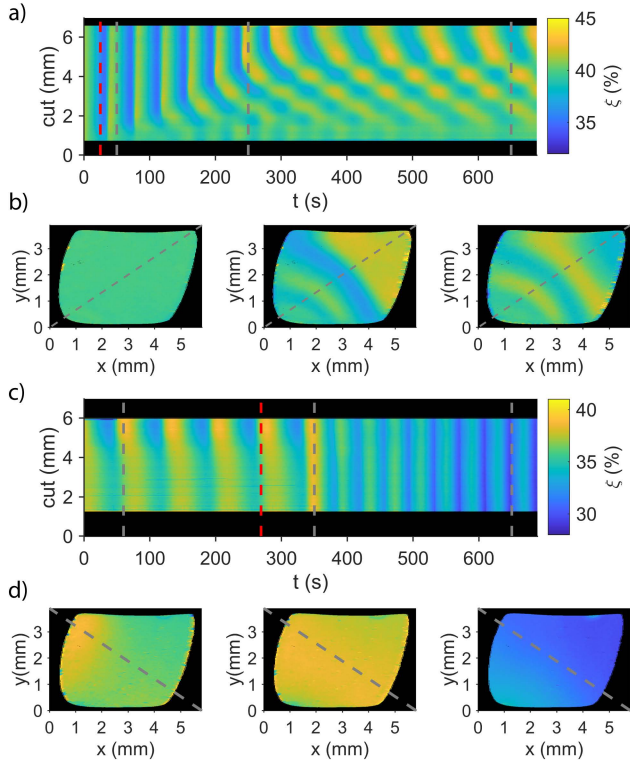
This is the author's peer reviewed, accepted manuscript. However, the online version of record will be different from this version once it has been copyedited and typeset.
PLEASE CITE THIS ARTICLE AS DOI: 10.1063/5.0064266



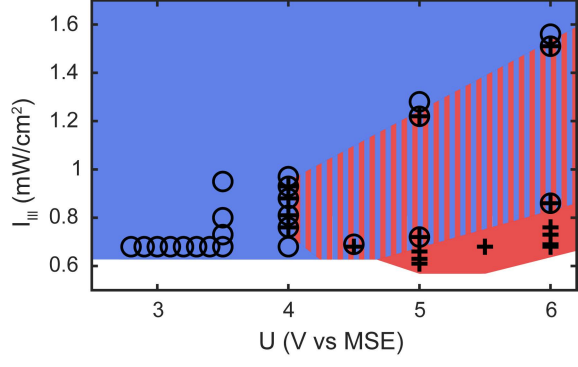
This is the author's peer reviewed, accepted manuscript. However, the online version of record will be different from this version once it has been copyedited and typeset.
PLEASE CITE THIS ARTICLE AS DOI: 10.1063/5.0064266



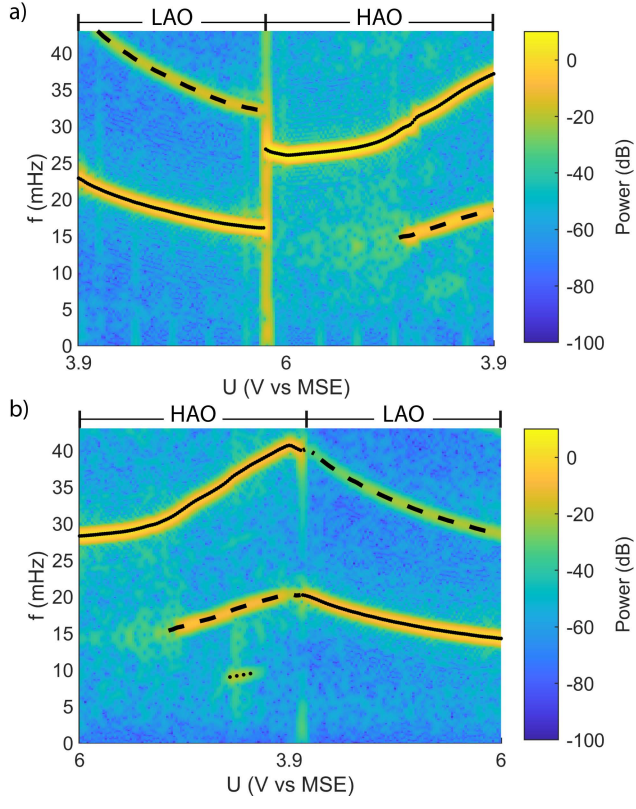
This is the author's peer reviewed, accepted manuscript. However, the online version of record will be different from this version once it has been copyedited and typeset.
 PLEASE CITE THIS ARTICLE AS DOI: 10.1063/5.0064266



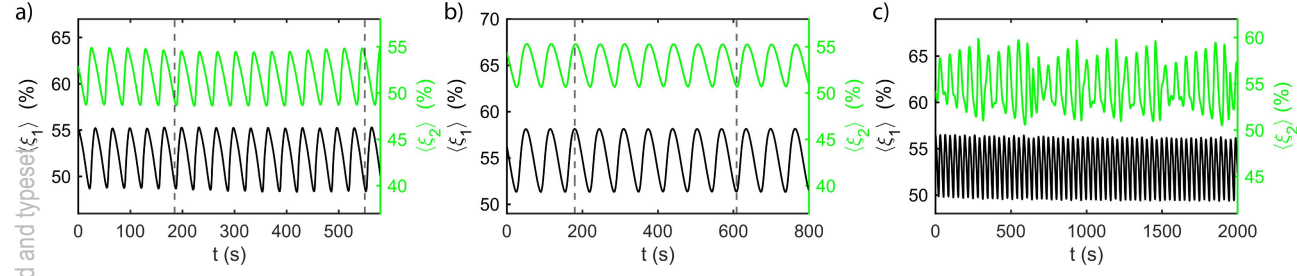
This is the author's peer reviewed, accepted manuscript. However, the online version of record will be different from this version once it has been copyedited and typeset.
PLEASE CITE THIS ARTICLE AS DOI: 10.1063/5.0064266



This is the author's peer reviewed, accepted manuscript. However, the online version of record will be different from this version once it has been copyedited and typeset.
 PLEASE CITE THIS ARTICLE AS DOI: 10.1063/5.0064266



This is the author's peer reviewed, accepted manuscript. However, the online version of record will be different from this version once it has been copyedited and typeset.
PLEASE CITE THIS ARTICLE AS DOI: 10.1063/5.0064266



This is the author's peer reviewed, accepted manuscript. However, the online version of record will be different from this version once it has been copyedited and typeset.
PLEASE CITE THIS ARTICLE AS DOI: 10.1063/5.0064266

